ELSEVIER

Fuel 80 (2001) 1535–1544

FUEL

www.fuelfirst.com

Heating and evaporation of semi-transparent diesel fuel droplets in the presence of thermal radiation

L.A. Dombrovsky[a], S.S. Sazhin[b,*], E.M. Sazhina[b], G. Feng[b], M.R. Heikal[b], M.E.A. Bardsley[c], S.V. Mikhalovsky[d]

[a]*Heat Transfer Department, Institute for High Temperatures of the Russian Academy of Sciences, Krasnokazarmennaya 17A, Moscow 111250, Russian Federation*

[b]*School of Engineering, University of Brighton, Cockcroft Building, Lewes Road, Brighton BN2 4GJ, UK*

[c]*Ricardo Consulting Engineers Ltd, Bridge Works, Shoreham-by-Sea, West Sussex BN43 5FG, UK*

[d]*School of Pharmacy and Biomolecular Sciences, University of Brighton, Cockcroft Building, Lewes Road, Brighton BN2 4GJ, UK*

Received 16 November 2000; revised 24 January 2001; accepted 24 January 2001

Abstract

Absorption and scattering spectral efficiency factors for spherical semi-transparent fuel droplets are approximated by simple analytical expressions as functions of imaginary and real parts of the complex index of refraction and the diffraction parameters of droplets. These expressions are applied to the modelling of thermal radiation transfer in Diesel engines. On the basis of the P-1 approximation, which is applicable due to the large optical thickness of combustion products, various ways of spectral averaging for absorption and scattering coefficients are suggested. Assuming that the concentration of fuel droplets is small, the scattering effects are ignored and the analysis is focused on approximations for the absorption coefficient. The average absorption coefficient of droplets is shown to be proportional to ar_d^{2+b}, where r_d is the droplet radii, and a and b are quadratic functions of gas temperature. Explicit expressions for a and b are derived for diesel fuel droplets in the range 5–50 μm and gas temperatures in the range 1000–3000 K. The expression for the average absorption coefficient of droplets is implemented into the research version of VECTIS CFD code of Ricardo Consulting Engineers. The effect of thermal radiation on heating and evaporation of semi-transparent diesel fuel droplets is shown to be considerably smaller when compared with the case of black opaque droplets.

Keywords: Diesel engines; Fuel droplets; Thermal radiation

1. Introduction

The contribution of thermal radiation to the heat transfer processes in Diesel engines has been widely discussed in the literature. In most models suggested so far, the contribution of thermal radiation heat transfer was taken into account via the absorption coefficient or emissivity of the multiphase medium, the value of which was a priori specified depending on soot concentration [1–9]. The contribution of fuel droplets per se to the process of thermal radiation transfer has been largely ignored. This assumption is justified when the overall energy balance in Diesel engines is considered [10], but it overlooks the effect of heating of droplets by thermal radiation which can contribute significantly to the process of droplet evaporation. The latter problem has been considered in a number of monographs and papers including Refs. [11–16].

The models suggested so far for radiative exchange between fuel droplets and gas can be subdivided into two main groups: those which take into account the transparency of droplets in the infrared range [11,12,14,15] and those which assume that droplets are grey opaque spheres [13,16]. The first group of models leads to a more accurate description of the process when compared with the second group of models, but at the expense of simplicity of formulation and computer efficiency. This complexity is not always justified in the multidimensional modelling of combustion processes in Diesel engines where the effects of thermal radiation are always secondary, when compared with conduction and convection (cf. modelling of the ignition process in a Diesel engine without the contribution of thermal radiation reported in Ref. [17]). Hence the interest in the second group of models, which are less accurate but can be more computer efficient.

* Corresponding author. Tel.: +44-1273-642677; fax: +44-1273-642301.

E-mail address: s.sazhin@brighton.ac.uk (S.S. Sazhin).

0016-2361/01/$ - see front matter
PII: S0016-2361(01)00025-4

The model suggested in this paper takes into account the transparency of fuel droplets but its formulation is considerably simpler when compared with the previously suggested models. This will allow us to attain a reasonable compromise between accuracy and computational efficiency. This is particularly important for the implementation of a thermal radiation model into a multidimensional computational fluid dynamics (CFD) code designed to model combustion processes in Diesel engines. Basic theory and approximations of the model are discussed in Section 2. In Section 3 the results are applied to the modelling of the processes of heating and evaporation of individual diesel fuel droplets where the contribution of thermal radiation is expected to be particularly important. The main results of the paper are summarized in Section 4.

2. Theory and approximations

The spectral radiation transfer equation for unpolarized radiation in a gas medium with particles of different sizes can be written in the form [14]:

$$\Omega\nabla I_\lambda(r,\Omega) + a_{\lambda(\mathrm{ext})} I_\lambda(r,\Omega) = \sum_i \frac{\sigma^i_{s\lambda(\mathrm{drop})}}{4\pi}\int I_\lambda(r,\Omega) f_i(\Omega\Omega')\,\mathrm{d}\Omega' + a_{\lambda(\mathrm{gas})}B_\lambda(T_\mathrm{g}) + \sum_i a^i_{\lambda(\mathrm{drop})i} B_\lambda(T_i), \quad (1)$$

where I_λ is the radiation intensity at a given point and at a given direction, $\mathrm{d}\Omega$ is the solid angle near the direction Ω, $a_{\lambda(\mathrm{gas})}$ is the absorption coefficient of gas, $a^i_{\lambda(\mathrm{drop})}$ and $\sigma^i_{s\lambda(\mathrm{drop})}$ are absorption and scattering coefficients of the ith droplet per unit volume, $a_{\lambda(\mathrm{ext})} = a_{\lambda(\mathrm{gas})} + \sum(a^i_{\lambda(\mathrm{drop})} + \sigma^i_{s\lambda(\mathrm{drop})})$ is the extinction coefficient, f_i is the scattering phase function of the ith droplet, $B_\lambda(T_{\mathrm{g}(i)})$ is the Planck function defined as [18]

$$B_\lambda(T_{\mathrm{g}(i)}) = \frac{C_1}{\pi\lambda^5[\exp(C_2/(\lambda T_{\mathrm{g}(i)})) - 1]},$$

$$C_1 = 3.742\times10^8\ \mathrm{W}\mu\mathrm{m}^4/\mathrm{m}^2, \qquad C_2 = 1.439\times10^4\ \mu\mathrm{m\ K}.$$

λ is the wavelength in μm.

In the presence of soot $a_{\lambda(\mathrm{gas})}$ includes the contributions of both gas and soot.

Eq. (1) can be simplified if we assume that f_i can be replaced by a sum of isotropic component and the component describing 'forward scattering' (transport approximation: see Ref. [14])

$$f_i(\mu_0) = (1-\bar\mu_i) + 4\pi\bar\mu_i\delta(1-\mu_0), \quad (2)$$

where $\mu_0 = \Omega\Omega'$, $\bar\mu_i$ (asymmetry factor of scattering) is defined as

$$\bar\mu_i = \frac{1}{4\pi}\int(\Omega\Omega')f_i(\Omega\Omega')\,\mathrm{d}\Omega'.$$

Having substituted Eq. (2) into Eq. (1) the latter equation can be simplified to

$$\Omega\nabla I_\lambda(r,\Omega) + a_{\lambda(\mathrm{tr})}I_\lambda(r,\Omega) = \frac{\sigma_{s\lambda(\mathrm{tr})}}{4\pi}I^0_\lambda(r) + a_{\lambda(\mathrm{gas})}B_\lambda(T_\mathrm{g}) + \sum_i a^i_{\lambda(\mathrm{drop})}B_\lambda(T_i), \quad (3)$$

where

$$I^0_\lambda(r) = \int I_\lambda(r,\Omega)\,\mathrm{d}\Omega.$$

$\sigma_{s\lambda\,(\mathrm{tr})} = \sum_i \sigma^i_{s\lambda\,(\mathrm{drop})}(1-\bar\mu_i)$ is the transport scattering coefficient, $a_\lambda = a_{\lambda\,(\mathrm{gas})} + \sum_i a^i_{\lambda\,(\mathrm{drop})}$, $a_{\lambda\,(\mathrm{tr})} = a_\lambda + \sigma_{s\lambda\,(\mathrm{tr})}$ is the transport extinction coefficient of the medium.

Integration of Eq. (3) over all solid angles gives

$$\nabla q_\lambda = 4\pi\left\{a_{\lambda(\mathrm{gas})}B_\lambda(T_\mathrm{g}) + \sum_i a^i_{\lambda(\mathrm{drop})}B_\lambda(T_i)\right\} - a_\lambda I^0_\lambda(r), \quad (4)$$

where

$$q_\lambda = \int I_\lambda(r,\Omega)\Omega\,\mathrm{d}\Omega$$

is the spectral radiation flux.

Eq. (4) will be analysed based on the so called P-1 approximation, widely used for analysis of thermal radiation transfer in Diesel engines [4,16]. In this approximation $q_\lambda = -1/(3a_{\lambda(\mathrm{tr})})\nabla I^0_\lambda(r)$ which allows us to rewrite Eq. (4) in the form

$$-\nabla\frac{1}{3a_{\lambda(\mathrm{tr})}}\nabla I^0_\lambda(r) + a_\lambda I^0_\lambda(r) = 4\pi\left((a_{\lambda(\mathrm{gas})}B_\lambda(T_\mathrm{g}) + \sum_i a^i_{\lambda(\mathrm{drop})}B_\lambda(T_i)\right). \quad (5)$$

Integration of both sides of Eq. (5) in the range between λ_1 and λ_2 gives

$$-\nabla\int_{\lambda_1}^{\lambda_2}\frac{1}{3a_{\lambda(\mathrm{tr})}}\nabla I^0_\lambda(r)\,\mathrm{d}\lambda + \int_{\lambda_1}^{\lambda_2}a_\lambda I^0_\lambda(r)\,\mathrm{d}\lambda = 4\pi\int_{\lambda_1}^{\lambda_2}\left((a_{\lambda(\mathrm{gas})}B_\lambda(T_\mathrm{g}) + \sum_i a^i_{\lambda(\mathrm{drop})}B_\lambda(T_i)\right)\mathrm{d}\lambda. \quad (6)$$

Let us assume that the dependence of radiation intensity on λ is close to that of a black body and introduce the following averaged values

$$\bar a_\mathrm{g} = \frac{\int_{\lambda_1}^{\lambda_2}a_{\lambda(\mathrm{gas})}(\lambda)B_\lambda(T_\mathrm{g})\,\mathrm{d}\lambda}{\int_{\lambda_1}^{\lambda_2}B_\lambda(T_\mathrm{g})\,\mathrm{d}\lambda} \approx \frac{\int_{\lambda_1}^{\lambda_2}a_{\lambda(\mathrm{gas})}(\lambda)I^0_\lambda\,\mathrm{d}\lambda}{\int_{\lambda_1}^{\lambda_2}I^0_\lambda\,\mathrm{d}\lambda}, \quad (7)$$

$$\bar{a}_i = \frac{\int_{\lambda_1}^{\lambda_2} a^i_{\lambda(\mathrm{drop})}(r_{\mathrm{d}i},\lambda)B_\lambda(T_\mathrm{g})\,\mathrm{d}\lambda}{\int_{\lambda_1}^{\lambda_2} B_\lambda(T_\mathrm{g})\,\mathrm{d}\lambda} \approx \frac{\int_{\lambda_1}^{\lambda_2} a^i_{\lambda(\mathrm{drop})}(r_{\mathrm{d}i},\lambda)I^0_\lambda\,\mathrm{d}\lambda}{\int_{\lambda_1}^{\lambda_2} I^0_\lambda\,\mathrm{d}\lambda}, \quad (8)$$

$$\tilde{a}_{\mathrm{tr}} = \frac{\int_{\lambda_1}^{\lambda_2} \left.\frac{\partial B_\lambda}{\partial T}\right|_{T=T_\mathrm{g}} \mathrm{d}\lambda}{\int_{\lambda_1}^{\lambda_2} \frac{1}{a_{\lambda(\mathrm{tr})}} \left.\frac{\partial B_\lambda}{\partial T}\right|_{T=T_\mathrm{g}} \mathrm{d}\lambda}. \quad (9)$$

When deriving Eq. (9) it was taken into account that

$$\nabla B_\lambda(T) = \frac{\partial B_\lambda}{\partial T}\nabla T.$$

If the range (λ_1,λ_2) is wide enough so that most radiation energy is concentrated in it we can write

$$\int_{\lambda_1}^{\lambda_2} B_\lambda(T_\mathrm{g})\,\mathrm{d}\lambda \approx \sigma T_\mathrm{g}^4/\pi.$$

Remembering the definition of the radiation temperature θ_R [19] we can write

$$\int_{\lambda_1}^{\lambda_2} I^0_\lambda\,\mathrm{d}\lambda \approx 4\sigma\theta_\mathrm{R}^4,$$

where σ is the Stefan–Boltzmann constant.

The combination of these approximate relations and Eqs. (7)–(9) allows us to simplify Eq. (6) to

$$\frac{1}{3}\nabla\frac{1}{\tilde{a}_{\mathrm{tr}}}\nabla\theta_\mathrm{R}^4 + \bar{a}_\mathrm{g}(T_\mathrm{g}^4 - \theta_\mathrm{R}^4) + \sum_i \bar{a}_i(T_i^4 - \theta_\mathrm{R}^4) = 0. \quad (10)$$

Using the Marshak boundary conditions [20,21] the normal component of the radiation heat flux at the boundaries q_n can be presented as

$$q_n = \frac{\sigma(T_w^4 - \theta_{\mathrm{R}w}^4)}{(1/\epsilon_w) - (1/2)}, \quad (11)$$

where T_w is the boundary temperature, ϵ_w is the emissivity of the boundary, $\theta_{\mathrm{R}w}$ is the radiation temperature at the boundary; when deriving Eq. (11) it was assumed that the boundaries are grey.

Once the distribution of θ_R in the domain has been found from Eq. (10) the thermal radiation heat flux can be estimated as [19]

$$q = -\frac{4\sigma}{3(a_\mathrm{g} + \sigma_{\mathrm{sg}})}\nabla\theta_\mathrm{R}^4. \quad (12)$$

An alternative approach to the application of the P-1 model to the case when fuel droplets are present in the system is based on the treatment of droplets' boundaries as any other boundaries, described by the emissivity of droplets' surfaces [16]. This treatment makes it necessary to write Eq. (10) for gas phase only and impose the Marshak boundary condition (11) at the droplets' surfaces. The driving force behind this approach was to treat droplets in exactly the same way as any other boundary with the characteristic scale equal to the size of droplets. The downside of this approach, however, is that in the case of optically thin medium the Marshak boundary conditions can lead to a considerable overestimation of the radiation flux near the surface of the sphere (cf. Figs. 15–11 in Ref. [21]) (this however, can be corrected by adjusting the value of ϵ_w). This approach cannot take into account the effect of droplets' scattering, which can dominate the absorption. Also, the semi-transparency of droplets in infrared range cannot be incorporated into this approach. Since both these effects have to be taken into account in the mathematical modelling of the interaction of thermal radiation with droplets, our analysis will be based on Eq. (10).

The values of $a^i_{\lambda(\mathrm{drop})}$ and $\sigma^i_{s\lambda(\mathrm{drop})}$ for individual droplets can be estimated as [14,22]

$$\{a^i_{\lambda(\mathrm{drop})}, \sigma^i_{s\lambda(\mathrm{drop})}\} = \frac{\pi r_{\mathrm{d}i}^2}{V}\{Q_{ai(\lambda)}, Q^{\mathrm{tr}}_{si(\lambda)}\}, \quad (13)$$

where $Q_{ai(\lambda)}$ and $Q^{\mathrm{tr}}_{si(\lambda)}$ are absorption and transport scattering efficiency factors for ith droplets, V is the volume of the computational cell (over which the summation in Eq. (4) is performed).

The values of $Q_{ai(\lambda)}$ and $Q^{\mathrm{tr}}_{si(\lambda)}$ can be calculated using the Mie scattering theory [14,22,23]. However, remembering the relatively minor role which thermal radiation plays in the heat balance in Diesel engines, an attempt to find reasonably accurate approximate expressions for Q_{ai} and Q^{tr}_{si} will be made below.

An approximate expression for $Q_{ai(\lambda)}$ have been suggested in the form [22]

$$Q_{ai(\lambda)} = 1 + \frac{\exp(-2\tau_i)}{\tau_i} - \frac{1 - \exp(-2\tau_i)}{2\tau_i^2}, \quad (14)$$

where $\tau_i = 2\kappa x_i$ is the optical thickness of liquid droplets, κ is the index of absorption of liquid droplets, and $x_i = 2\pi r_{\mathrm{d}i}/\lambda$ is the diffraction parameter of droplets.

Approximation (14) is valid for spherical droplets when $x_i \gg 1$, $|n-1| \ll 1$ (n is the index of refraction), and $\kappa \ll 1$. Remembering that $\kappa = k_\lambda\lambda/4\pi$, where k_λ is the absorption coefficient [24], we can simplify the expression for τ_i to $\tau_i = k_\lambda r_{\mathrm{d}i}$.

In the case of large optically soft cylinders one can write

$$Q_{ai(\lambda)} = 1 - \exp(-2\tau_i). \quad (15)$$

As will be shown later approximation (15) is applicable to spherical droplets in a certain range of indices of refraction.

To assess the range of applicability of approximations (14) and (15) the predictions of these formulae are compared with the predictions of the Mie theory for $\kappa = 0.01$ and a range of values of n. The results are shown in Fig. 1. As can be seen from this figure, approximation (14) is acceptable for the case when $n = 1.01$, but turns out to be poor for other values of n. On the other hand, for n in the range $1.3 \le n \le 1.5$, the simple approximation (15) gives reasonably accurate results.

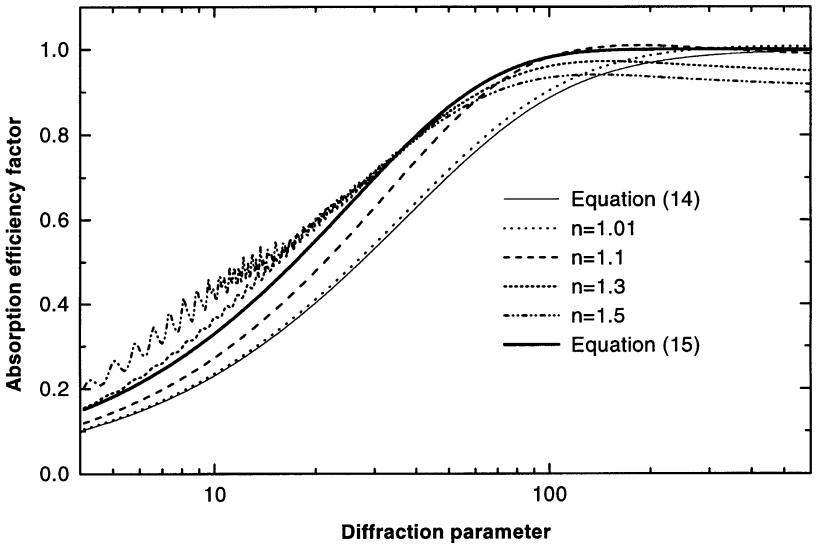

Fig. 1. Absorption efficiency factor (Q_{ai}) versus diffraction parameter (x_i) as predicted by Eq. (15) (thick solid), Eq. (14) (thin solid), and the Mie theory for $n = 1.01$ (dotted), $n = 1.1$ (dashed), $n = 1.3$ (short dashes), and $n = 1.5$ (long dashes) for the index of absorption $\kappa = 0.01$.

In Fig. 2 predictions of Eq. (15) are compared with the predictions of the Mie theory in a wider range of parameters κ and x_i, typical for diesel fuel droplets. As follows from this figure, the error introduced by Eq. (15) is typically less than about 10% which is acceptable for practical applications to modelling combustion processes in Diesel engines.

Restricting the analysis to the case when x_i is sufficiently large ($x_i \gg 10$) we approximated $Q^{\mathrm{tr}}_{si(\lambda)}$ by the following expression:

$$Q^{\mathrm{tr}}_{si(\lambda)} = A\left(\frac{10}{x_i}\right)^q, \tag{16}$$

where

$$A = 1 - \kappa^{0.13};$$

$$q = \frac{4}{(\log_{10}\kappa)^2}[1 + 2(1.5 - n)\exp(-200\kappa)].$$

Approximation (16) is certainly not unique. The power dependence of $Q^{\mathrm{tr}}_{si(\lambda)}$ on x_i, however, is convenient for integration of this function for a polydisperse spray.

A comparison between the predictions of Eq. (16) and the results predicted by the Mie theory for the same values of parameters as in Fig. 2 is shown in Fig. 3. As can be seen from this figure, Eq. (16) gives a reasonably accurate approximation for $Q^{\mathrm{tr}}_{si(\lambda)}$ for $\kappa = 10^{-2}$. In the case of smaller

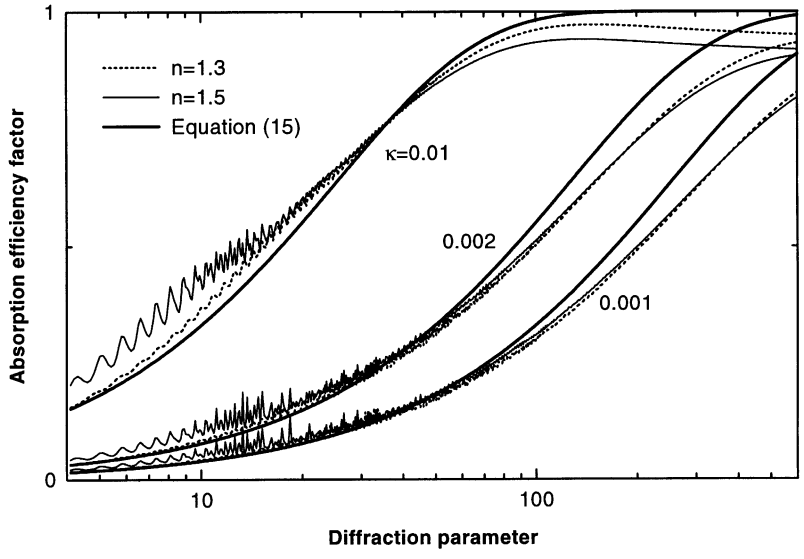

Fig. 2. Absorption efficiency factor (Q_{ai}) versus diffraction parameter (x_i) as predicted by Eq. (15) (thick solid), and the Mie theory for $n = 1.3$ (short dashes), and $n = 1.5$ (thin solid) for $\kappa = 0.01$, $\kappa = 0.002$, and $\kappa = 0.001$ (indicated near the curves).

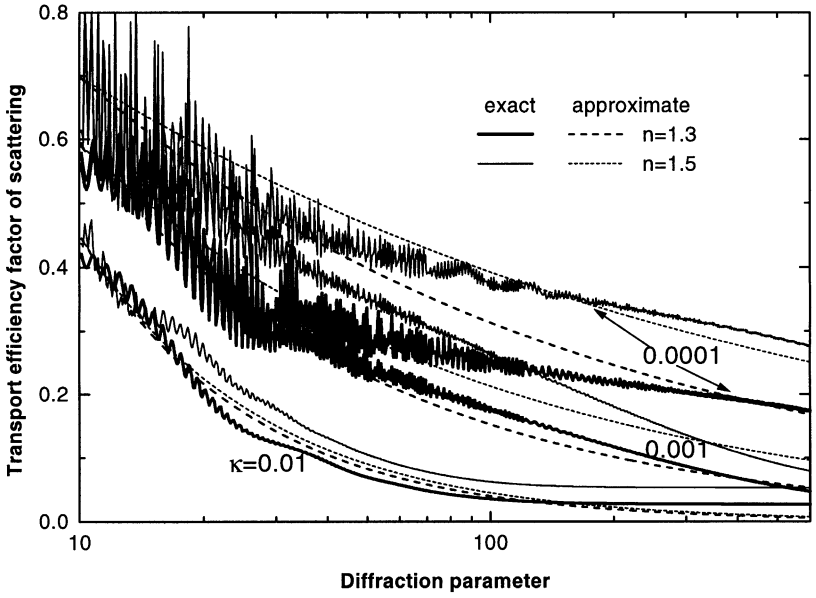

Fig. 3. Transport efficiency factor of scattering (Q_{si}^{tr}) versus diffraction parameter (x_i) as predicted by Eq. (16) for $n = 1.3$ (thick solids), and $n = 1.5$ (thin solids) and the Mie theory for $n = 1.3$ (long dashes), and $n = 1.5$ (short dashes) for $\kappa = 0.01$, and $\kappa = 0.0001$ (indicated near the curves).

κ the error introduced by Eq. (16) increases. In all cases, however, approximation (16) describes the main features of $Q_{si(\lambda)}^{tr}$ and gives a correct value of its order of magnitude.

Note that the error of approximation (16) for polydisperse systems of fuel droplets would be less than that for monodisperse droplets (this follows directly from Mie calculations which are not presented in this paper). Approximations (15) and (16) can be used in the limited range of parameters. This range, however, includes the range of parameters appropriate for modelling combustion of fuel in Diesel engines.

The dependence of κ on λ in the range (0.2 μm, 16 μm) for diesel fuel is shown in Fig. 4. Comparing Fig. 4 with the corresponding figure for *n*-decane presented in Refs. [25,26] one can see that in both cases the peaks of absorptivity near $\lambda = 4$ μm and $\lambda = 8$ have been observed. A number of peaks in diesel fuel spectra cannot be easily identified and can be related to various additives. Based on the results reported in [25,26] we can conclude that n changes in the range from 1.1 to 1.8 for wavelengths in the range (2 μm, 16 μm). As a zeroth approximation we will assume that $n = 1.45$. We can anticipate that the range of n for diesel fuel is similar, although we were not able to perform direct measurements of these parameters.

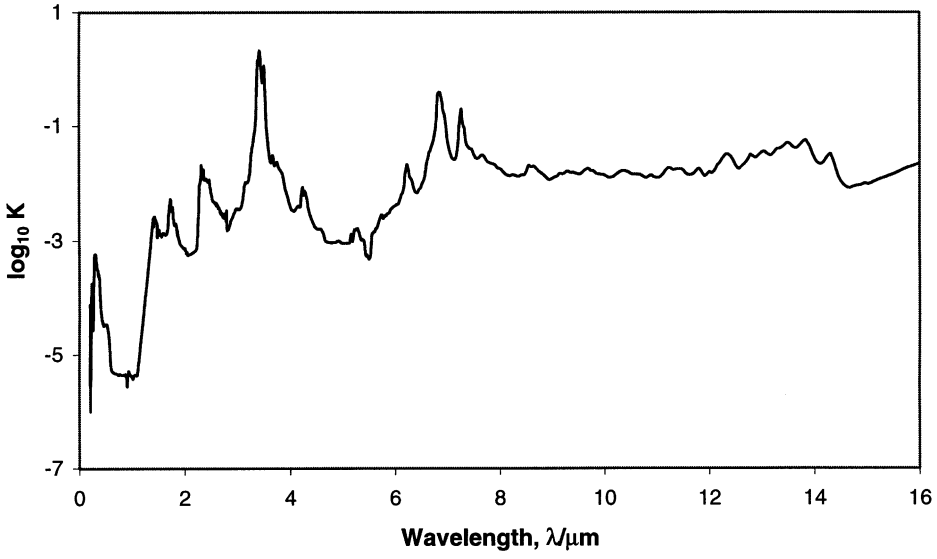

Fig. 4. Index of absorption of diesel fuel versus wavelength λ.

The choice of λ_1 and λ_2 can be made based on the wavelength at which the intensity of thermal radiation is maximal, the availability of data for κ and the level of absorption of infrared radiation. This wavelength at which the intensity of thermal radiation is maximal can be found from the Wien's displacement law [18]

$$\lambda_{\max} = \frac{C_3}{T_g}, \tag{17}$$

where $C_3 = 2897.8$ μm K, $\lambda_{\max}$ is measured in μm.

The value of λ_1 is taken equal to 1 μm. Although the level of radiation at $\lambda < 3$ μm can be substantial its contribution to the absorption by the droplets is expected to be small due to small value of κ (see Fig. 4). The value of λ_2 is taken equal to 6 μm. At larger λ the intensity of radiation is expected to be small. Note that the model developed in this paper is not applicable to the case when the wavelength is greater than the droplets' diameter. Hence, the contribution of the waves with wavelengths greater than 6 μm would restrict the range of applicability of the model.

As follows from Fig. 4, the index of absorption approaches 1 at λ close to 4 μm. At the same time our approximate expressions are strictly valid for $\kappa \le 0.01$. We may ignore the limitation $\kappa \le 0.01$ in the case of $\kappa < 0.02 - 0.03$. In the case of $\kappa > 0.1$, the dependence of Q_{ai} on the diffraction parameter is usually non-monotonic and it is not described by Eq. (15). The range of λ when $\kappa > 0.1$, however, is rather narrow and we do not expect that ignoring this limitation would introduce a substantial error in the final results after the integration over all λ.

Our analysis will be based on Eq. (10). In this equation we assume that $\bar{a}_g$, which is mainly controlled by soot, is a priori given or taken from the experiment. The combination of Eqs. (8), (9) and (13) allows us to present expressions for $\bar{a}_i$ and $\tilde{a}_{tr}$ in the forms

$$\bar{a}_i = \frac{\pi r_{di}^r}{V} \frac{\int_{\lambda_1}^{\lambda_2} Q_{ai(\lambda)} B_\lambda(T_g)\, d\lambda}{\int_{\lambda_1}^{\lambda_2} B_\lambda(T_g)\, d\lambda}, \tag{18}$$

$$\tilde{a}_{tr} = \frac{\int_{\lambda_1}^{\lambda_2} \frac{B_\lambda(T_g)}{\lambda} \exp\left(\frac{C_2}{\lambda T_g}\right) d\lambda}{\int_{\lambda_1}^{\lambda_2} \frac{B_\lambda(T_g)}{\lambda a_{\lambda(tr)}} \exp\left(\frac{C_2}{\lambda T_g}\right) d\lambda}, \tag{19}$$

where $a_{\lambda(tr)} = a_{\lambda(gas)} + \sum_i \frac{\pi r_{di}^2}{V}[Q_{ai(\lambda)} + Q_{si(\lambda)}^{tr}]$, a_{gas} is the absorption coefficient of gas and soot (assumed to be independent of λ as the zeroth approximation: cf.[27]).

When deriving Eq. (19) dB_λ/dT has been presented in an explicit form.

As a zeroth approximation we can assume that $a_{\lambda(gas)} \gg \sum_i \pi r_{di}^2/V[Q_{ai(\lambda)} + Q_{si(\lambda)}^{tr}]$. This allows us to replace $\tilde{a}_{tr}$ by $\bar{a}_{gas}$, where the main contribution to $\bar{a}_{gas}$ comes from soot. This assumption is justified for the parameters corresponding to a diesel spray.

Remembering Eq. (15) and the definition of B_λ, expression for $\bar{a}_i$ can be presented in a more explicit form

$$\bar{a}_i = \frac{\pi r_{di}^2}{V} \Lambda, \tag{20}$$

where

$$\Lambda = 1 - \frac{\int_{\lambda_1}^{\lambda_2} \frac{\exp\left(-\frac{8\pi\kappa r_{di}}{\lambda}\right)}{\lambda^5[\exp(C_2/(\lambda T_g)) - 1]} d\lambda}{\int_{\lambda_1}^{\lambda_2} \frac{d\lambda}{\lambda^5[\exp(C_2/(\lambda T_g)) - 1]}}, \tag{21}$$

the value of C_2 has been defined earlier.

As follows from Eq. (20), the maximal values of $\bar{a}_i = (\pi r_{di}^2)/V$ are achieved when κ is sufficiently large over the whole spectral range. For small κ, $\bar{a}_i$ is expected to be close to zero. For effective implementation of the expression for $\bar{a}_i$ into a CFD code we need to find a reasonably accurate but simple approximation of the function $\Lambda(r_{di}, T_g)$.

This approximation is expected to be applicable to numerical modelling of the processes of heating and evaporation of diesel fuel droplets, which are the integral part of the diesel combustion processes. Radii of these droplets are expected to be mainly less than 50 μm [28,29]. Gas temperature is not expected to exceed about 3000 K.

Taking into account the function $\kappa(\lambda)$ shown in Fig. 4, and having tried various approximations we have found that the best approximation for Λ in the ranges $5 \le r_{di} \le 50$ μm and 1000 K $\le T_g \le$ 3000 K is provided by the function

$$\Lambda_0 = a r_{di}^b, \tag{22}$$

where

$$a = 0.095268 - 0.049415(T_g/1000) + 0.0072018(T_g/1000)^2,$$

$$b = 0.38947 + 0.13089(T_g/1000) - 0.014647(T_g/1000)^2.$$

T_g is measured in K, r_{di} is measured in μm.

The contribution of thermal radiation for $T_g < 1000$ K is negligibly small in most cases. As can be seen, a decreases about five times when T_g increases from 1000 to 3000 K. The dependence of b on T_g is much slower: it increases from about 0.51–0.65 when T_g increases from 1000 to 3000 K.

The comparison between the plots $\Lambda(r_{di})$ and $\Lambda_0(r_{di})$ for T_g in the range between 1000 and 3000 K is shown in Fig. 5. As can be seen from this figure, the coincidence between the plots appears to be almost ideal. This enables us to apply, with confidence, Λ_0 instead of Λ for numerical computations of the processes of heating and evaporation of fuel droplets as part of the combustion process in Diesel engines. Some specific applications of this approach will be considered in Section 3.

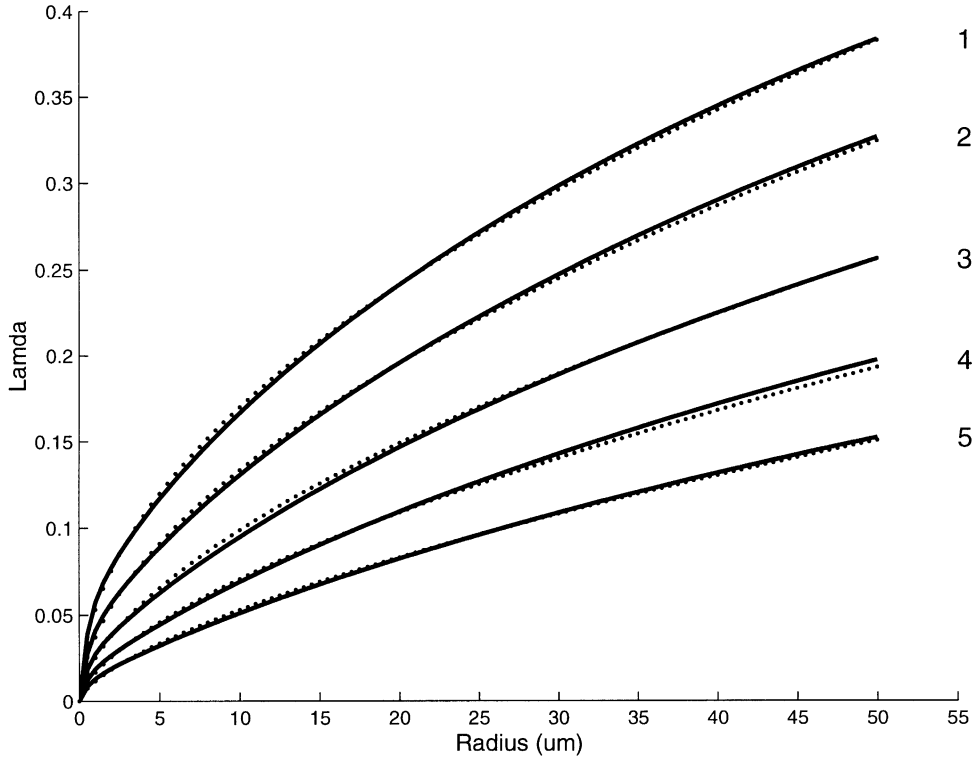

Fig. 5. Plots of Λ versus r_{di} (solid) and Λ_0 versus r_{di} (dotted) for $T_g = 1000$ K (curve 1), $T_g = 1500$ K (curve 2), $T_g = 2000$ K (curve 3), $T_g = 2500$ K (curve 4) and $T_g = 3000$ K (curve 5). r_{di} is in μm.

Note that the plots Λ_0 and Λ are not reliable at $r_{di} <$ 6 μm. However, since the relative contribution of droplets with $r_{di} < 6$ μm is small in Diesel engines, it is not expected that this restriction will effect the results of computer modelling of combustion processes in Diesel engines in a significant way.

3. Applications

To illustrate the importance of the effects described in Section 2, expression (20) for $\bar{a}_i$, with $\Lambda = \Lambda_0$ as defined by Eq. (22), has been implemented into the research version of VECTIS CFD code. This code was developed by Ricardo Consulting Engineers with particular attention given to the requirements of automotive applications. It combines the Eulerian gas flow model and the Lagrangian spray model. It uses Cartesian grid with local refinements and all equations are solved in three dimensions.

A single droplet has been placed in the centre of a cube filled by a hot gas, the temperature of which was taken equal to the temperature of the walls. The droplet was not moving and no initial gas flow has been specified. The size of the domain ensured that the average gas temperature remained almost constant; the grid size has been set equal to 0.5 mm.

Values of parameters typical for Diesel engine have been taken: gas pressure p has been taken equal to 6 MPa, droplet initial temperature and diameter have been taken equal to 300 K and 50 μm, respectively, the temperature of gas has been taken equal to 1500 K. Plots of droplet temperature and diameter as functions of time are shown in Fig. 6a and b. These plots refer to the cases when the effects of thermal radiation are ignored altogether, when the thermal radiation is accounted for based on Eqs. (20) and (22) (semi-transparent droplets), and when thermal radiation is accounted for based on Eq. (20) with $\Lambda = 1$ (black opaque droplets). As follows from Fig. 6a, the effect of thermal radiation on semi-transparent droplets is noticeably smaller when compared with this effect on black opaque droplets. In the case of black droplets their temperature reached the critical value of 726 K for diesel fuel when their diameter dropped to about 25 μm. This effect has not been observed in the case of semi-transparent droplets when the temperature remained subcritical all way through (until droplets evaporated). The difference between black and semi-transparent droplets is even more clearly seen in Fig. 6b. The initial increase of droplet diameters is due to droplets' thermal expansion. For realistic semi-transparent droplets the effects of radiation would lead to a small (about 3%) decrease of their evaporation time when compared with the case without thermal radiation. Note that in the case when Marshak's boundary conditions were imposed on the droplet surfaces, the effect of thermal radiation could become even stronger when compared with the black droplets ($\Lambda = 1$). Hence, this approach would lead to even less accurate prediction of the effect of thermal radiation on

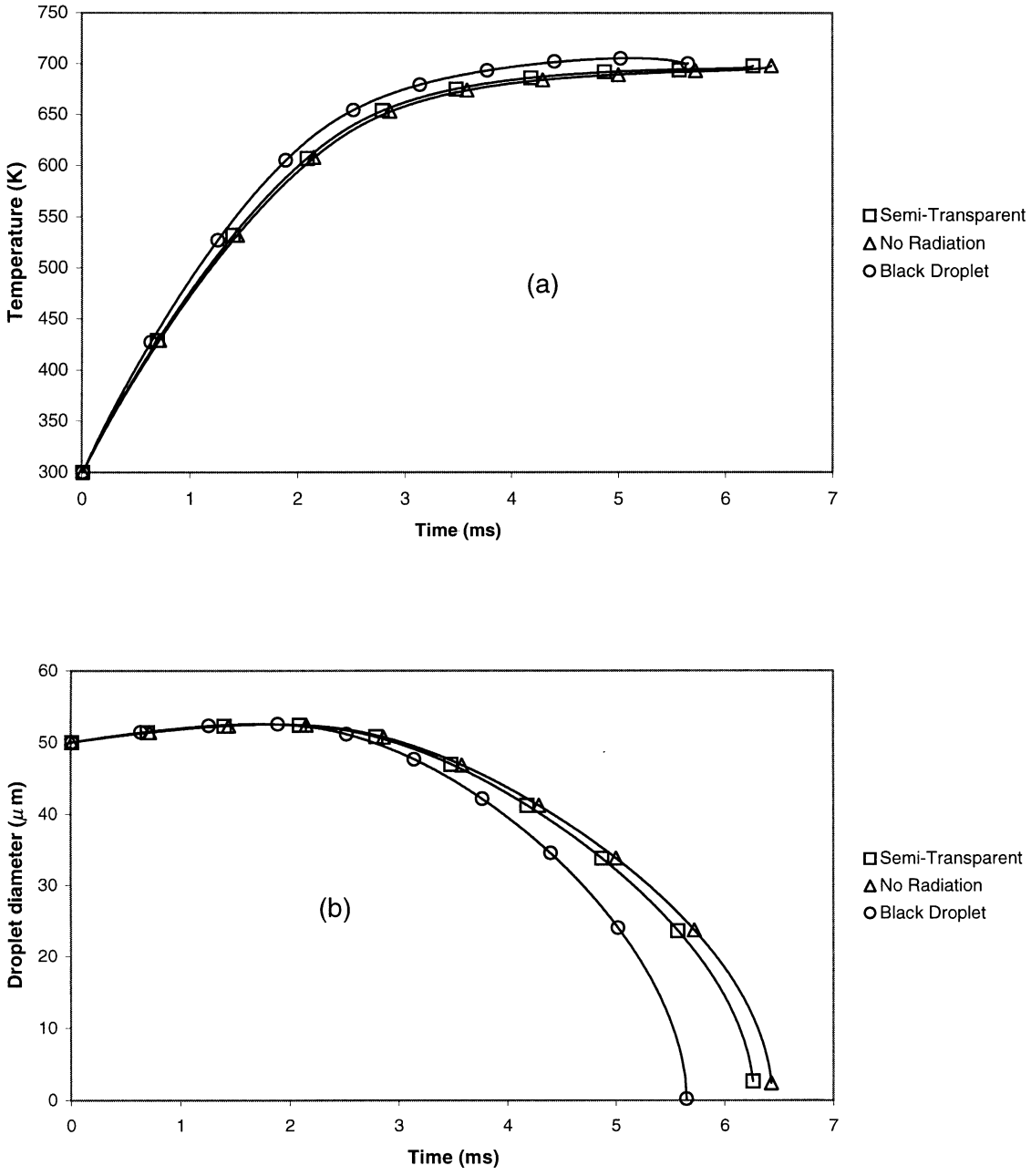

Fig. 6. Plots of droplet temperatures versus time (a) and droplet diameter versus time (b) for the cases when the effects of thermal radiation have been ignored, taken into account based on Eqs. (20) and (22) (semi-transparent droplets), and taken into account based on Eq. (20) with $\Lambda = 1$ (black opaque droplets). The initial droplet temperature and diameter are taken equal to 300 K and 50 μm, respectively, the gas (air) temperature and pressure are taken equal to 1500 K and 6 MPa, respectively.

realistic semi-transparent droplets when compared with black droplets.

Results similar to those shown in Fig. 6 have been obtained for other temperatures in the range 1500–2500 K and droplet diameters in the range 20–50 μm. As expected, the effects of thermal radiation and the difference between the cases of black and semi-transparent droplets became more prominent for larger droplets and larger gas temperatures. Based on these results we could conclude that thermal radiation leads to a more rapid heating of semi-transparent droplets and reduction of their evaporation times. These effects, however, are considerably weaker than similar effects for black opaque droplets.

4. Conclusions

(a) Simple analytical expressions have been suggested to

approximate absorption and transport spectral efficiency factors for spherical semi-transparent droplets. These expressions have been shown to be in reasonable agreement with the predictions of the Mie theory.

(b) These expressions have been used for calculation of average (over wavelengths in a given range) absorption and transport coefficients. The latter, in turn, have been used in the P-1 model, which has been applied to the modelling of the thermal radiation transfer in Diesel engines in the presence of liquid fuel droplets.

(c) Assuming that the concentration of droplets is small and the absorption of the soot-laden mixture is large, the effects of droplets on thermal radiation transfer has been reduced to the exchange of radiative energy between droplets and gas.

(d) The average absorption coefficient of droplet has been approximated as a function proportional to ar_d^{2+b}, where r_d is the droplet radius, a and b are polynomials of the second order of gas temperature. Explicit expressions for a and b have been found for diesel fuel droplet radii in the range 5–50 μm and gas temperatures in the range 1000–3000 K.

(e) The average absorption coefficient in this form has been implemented into the research version of VECTIS CFD code of Ricardo Consulting Engineers with the P–1 thermal radiation model. It has been shown that the effect of thermal radiation on heating and evaporation of realistic semi-transparent diesel fuel droplets is considerably smaller when compared with the case when droplets are approximated as black opaque spheres. This means that the latter approximation, sometimes used in numerical modelling of radiative transfer between droplets and gas can be poor and needs to be replaced by the approximation suggested in the paper. This approximation combines the simplicity and reasonable accuracy required for modelling thermal radiation transfer within the framework of numerical modelling of combustion processes in Diesel engines.

Acknowledgements

The authors are grateful to Ricardo Consulting Engineers for the technical and financial support of this project.

Appendix A. Measurements of the index of absorption of diesel fuel

The index of absorption of diesel fuel has been measured in ultraviolet, visible and infrared regions. The ultraviolet and visible parts have been investigated using Unicam 'HEλIOS β' UV-visible spectrometer (model 2.03) in a quartz cell with optical path equal to 1 cm in the range 0.2–1.2 μm. The infrared part of the spectrum has been investigated using FTIR (Fourier transform infrared) spectrometer Perkin–Elmer 1720-X with the 4 cm^{-1} resolution in the range of 7200–600 cm^{-1} (1.39–16.7 μm) in NaCl cell of 0.011 mm optical path. Due to strong absorption in the ranges 3.3–3.6 and 6.8–6.9 μm diesel fuel has been diluted with carbon tetrachloride and the necessary correction for this dilution has been made.

All measurements have been carried out at room temperature. The index of absorption in ultraviolet and visible regions is almost independent of temperature, whereas in the infrared region additional 'hot bands' may appear at high temperatures resulting in the overall increase of absorption [30].

References

[1] Kunitomo T, Matsuoka K, Oguri T. Prediction of radiative heat transfer in a Diesel engine. SAE technical paper 750786, 1975.
[2] Chang SL, Rhee KT. Computation of radiation heat transfer in Diesel combustion. SAE technical paper 831332, 1983.
[3] Chapman M, Friedman MC, Aghan A. A time-dependent spatial model for radiant heat transfer in Diesel engines. SAE technical paper 831725, 1983.
[4] Mengüç MP, Viskanta R, Ferguson CR. Multidimensional modelling of radiative heat transfer in Diesel engines. SAE technical paper 850503, 1985.
[5] Viskanta R, Mengüç MP. Radiation heat transfer in combustion systems. Prog Energy Combust Sci 1987;13:97–160.
[6] Wahiduzzaman S, Morel T, Timar J, DeWitt DP. Experimental and analytical study of heat radiation in a Diesel engine. SAE technical paper 870571, 1987.
[7] Cheung CS, Leung CW, Leung TP. Modelling spatial radiative heat flux distribution in a direct injection Diesel engine. Proc Inst Mech Engng 1994;208:275–83.
[8] Abraham J, Magi V. Modelling radiant heat loss characteristics in a Diesel engine. SAE technical paper 970888, 1997.
[9] Furmański P, Banaszek J, Wiśnewski T, Rebow M. Influence of thermal radiation from the burned zone on heat transfer in the piston of Diesel engine. In: Groshal B, Mikielewicz J, Sunden B, editors. Progress in Engineering Heat Transfer. IFFM Publishers. Proceedings of 3rd Baltic Heat Transfer Conference. Gdańsk, Poland, 22–24 September 1999; p. 11–8.
[10] Flynn PF, Durrett RP, Hunter GL, zur Loye AO, Akinyemi OC, Dec JE, Westbrook CK. Diesel combustion: an integrated view combining laser diagnostics, chemical kinetics, and empirical validation. SAE report 1999-01-0509, 1999.
[11] Lage PLC, Rangel RH. Single droplet vaporization including thermal radiation absorption. J Thermophys Heat Transfer 1993;7(3):502–9.
[12] Chang K-C, Shieh J-S. Theoretical investigation of transient droplet combustion by considering flame radiation. Int J Heat Mass Transfer 1995;14:2611–21.
[13] Marchese AJ, Dryer FL. The effect of non-luminous thermal radiation in microgravity droplet combustion. Combust Sci Technol 1997;124:371–402.
[14] Dombrovsky LA. Radiation heat transfer in disperse systems. New York, Wallingford (UK): Begell House, 1996.
[15] Dombrovsky LA. Thermal radiation from non-isothermal spherical particles of a semitransparent material. Int J Heat Mass Transfer 2000;43:1661–72.
[16] Sazhin SS, Sazhina EM, Heikal MR. Modelling of the gas to fuel droplets radiative exchange. Fuel 2000;79:1843–52.
[17] Sazhina EM, Sazhin SS, Heikal MR, Babushok VI, Johns R. A detailed modelling of the spray ignition process in diesel engines. Combust Sci Technol 2000;160:317–44.

[18] Incropera FP, de Witt D. Fundamentals of heat and mass transfer. New York: Wiley, 1990.
[19] Sazhin SS, Sazhina EM, Faltsi-Saravelou O, Wild P. The P-1 model for thermal radiation transfer (advantages and limitations). Fuel 1996;75(3):289–94.
[20] Marshak RE. Note on the spherical harmonic method as applied to the Milne problem for a sphere. Phys Rev 1947;71(7):443–6.
[21] Siegel R, Howell JR. Thermal radiation heat transfer. Washington: Hemisphere, 1992.
[22] Van de Hulst HC. Light scattering by small particles. New York: Wiley, 1957.
[23] Bohren CF, Huffman DR. Absorption and scattering of light by small particles. New York: Wiley, 1983.
[24] Born M, Wolf E. Principles of optics. New York: Pergamon Press, 1975.
[25] Tuntomo A. Transport phenomena in a small particle with internal radiant absorption. PhD thesis, University of California at Berkeley, 1990.
[26] Lage PLC, Rangel RH. Total thermal radiation absorption by a single spherical droplet. J Thermophys Heat Transfer 1993;7(1):101–9.
[27] Sazhin SS, Sazhina EM. The effective emissivity approximation for the thermal radiation transfer problem. Fuel 1996;74(14):1646–54.
[28] Pitcher G, Wigley G, Saffman M. Velocity and drop size measurements in fuel sprays in a direct injection Diesel engine. Particle and Particle Syst Charact 1990;7:160–8.
[29] Comer M. Transient G-DI fuel spray characterisation. PhD thesis, University of Wales, Cardiff, 1999.
[30] Hollas JM. Modern spectroscopy. 3rd ed. New York: Wiley, 1996.